

## **A Versatile and High-throughput Flow-cell System Combined with Fluorescence Imaging for Simultaneous Single-Molecule Force Measurement and Visualization**

Zhenyu Zou <sup>‡ a,b</sup>, Jialun Liang <sup>‡ a,b</sup>, Qian Jia <sup>c</sup>, Di Bai <sup>d</sup>, Wei Xie <sup>c</sup>, Wenqiang Wu <sup>d</sup>,  
Chuang Tan\* <sup>a,b</sup> and Jie Ma\* <sup>a,b</sup>

<sup>a</sup> School of Physics, Sun Yat-sen University, Guangzhou 510275, P.R. China.

<sup>b</sup> State Key Laboratory of Optoelectronic Materials and Technologies, Sun Yat-sen University, Guangzhou 510275, P.R. China.

<sup>c</sup> MOE Key Laboratory of Gene Function and Regulation, State Key Laboratory for Biocontrol, School of Life Sciences, Sun Yat-Sen University, Guangzhou, Guangdong, 510006, P.R. China.

<sup>d</sup> School of Life Sciences, State Key Laboratory of Crop Stress Adaptation and Improvement, Henan University, Kaifeng 475001, P.R. China

<sup>‡</sup> These authors contributed equally to this work.

\*Corresponding authors: majie6@mail.sysu.edu.cn; tanch26@mail.sysu.edu.cn.

## Section S1. Details of preparing DNA template

### (i) Preparation of DNA Constructs for overstretching

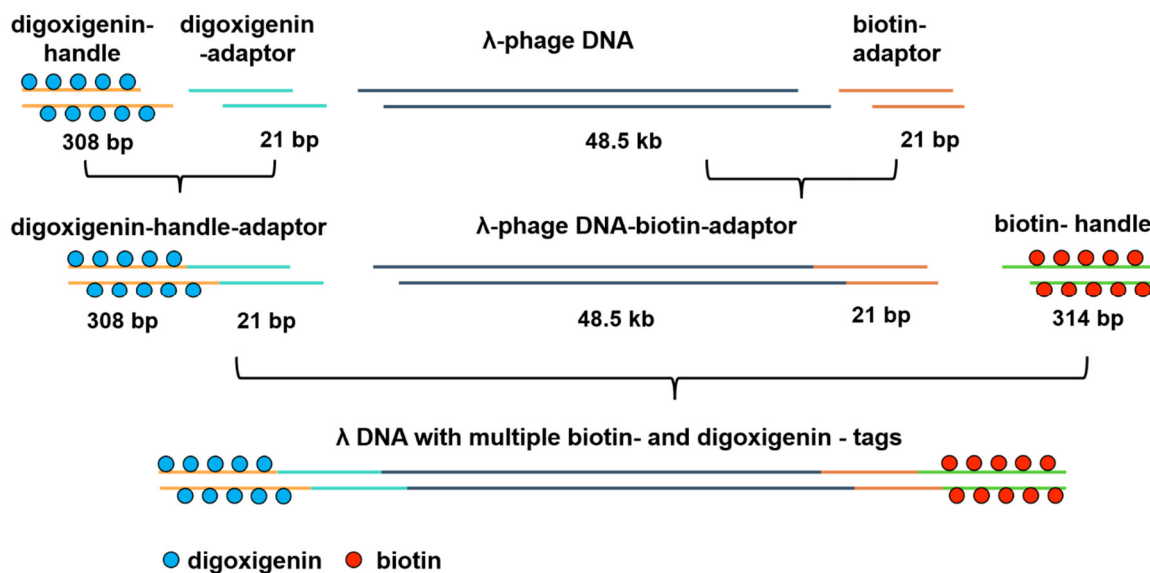


**Fig. S1** Schematic of synthesis of lambda DNA with multiple biotin- and digoxigenin-tags at each end.

The lambda DNA template with multiple biotin- and digoxigenin-tags at each end was synthesized as previously described<sup>1</sup>. The outline of the preparation process is shown in Fig. S1. Briefly, the template was constructed from 5 parts: digoxigenin-handle, digoxigenin-adaptor, lambda-phage DNA, biotin-adaptor, and biotin-handle. Both biotin- and digoxigenin-labeled handles were produced by amplifying a 329-bp fragment from the plasmid pJM1 (sequence available upon request) through a polymerase chain reaction (PCR) with forward primer HAF4 and reverse primer HBR4 (see Table S1). The PCR was carried out with 1/3 of dTTP replaced by biotin-16-dUTP (Roche, 11093070910) or digoxigenin-11-dUTP (Roche, 11093088910), respectively. After PCR, the biotin-handle was digested via BsaI (NEB, R3733S) at 37 °C for 3 hours to generate a 314-bp DNA segment with 4-nt sticky end; while the digoxigenin-handle was digested via BbsI (NEB, R3539S) at 37 °C for 3 hours resulting in a 308-bp DNA segment with 4-nt overhang. The digoxigenin-handle was then ligated to digoxigenin-adaptor, which was prepared by annealing designed dig adaptor oligo 1 and 2 (see

Table S1), at 1:3 molar ratio at 16 °C overnight. The ligation product was purified via PureLink PCR purification kit (Invitrogen, K310001) to get rid of the excess digoxigenin-adaptors. Lambda-DNA (NEB, N3011S) was ligated with the biotin-adaptor, which was generated by annealing designed biotin adaptor oligo 1 and 2 (see Table S1) at 1:10 molar ratio overnight. The excess biotin-adaptors were removed through ultrafiltration (Amicon, UFC505024). Finally, the digested biotin-handle, the ligation product of digoxigenin handle with the digoxigenin-adaptor and the ligation product of lambda-phage DNA with the biotin-adaptor were mixed at 3:2:1 molar ratio and ligated together to get the final lambda DNA template with multiple biotin and digoxigenin tags at each end. T4 DNA ligase (NEW ENGLAND BioLabs, N3011S) was used in all the ligation reactions.

**(ii) Preparation of DNA Constructs for T7 RNAP transcription**

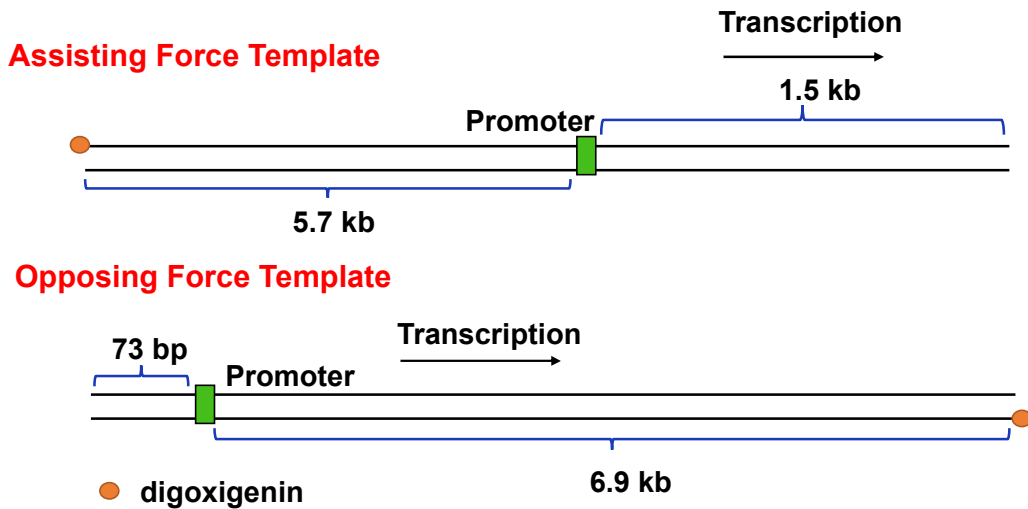


**Fig S2** Schematic of transcription templates.

Two kinds of DNA constructs were prepared for T7 RNAP transcription experiments (Fig. S2). Both the DNA templates were amplified from plasmid pJM2 by PCR via KOD FX DNA polymerase (Toyobo, KOD-101) using different primers (see Table S1). The digoxigenin tag in the template was introduced by a 5' digoxigenin-labeled primer. Notably, the sequence of 1500 bases downstream of the promoter was the same for the "assisting-force" template and the "opposing-force" template. To form

the stable paused transcription complex (PTC), the first 15 bases of the nascent RNA after the promoter were designed to contain only three kinds of nucleotides (G, A and C), *i.e.*, 5' TAATACGACTCACTATAGGGGGAGACCACAACGGT 3'<sup>2</sup>. With only GTP, CTP and ATP nucleotides introduced, RNAP started RNA synthesis from the underlined “G” and stopped at the underlined “T”. The transcription can be resumed later in the single-molecule experiment by introducing four kinds of nucleotides (GTP, ATP, CTP and UTP).

### (iii) Preparation of DNA Constructs for DNA hairpin hopping experiment

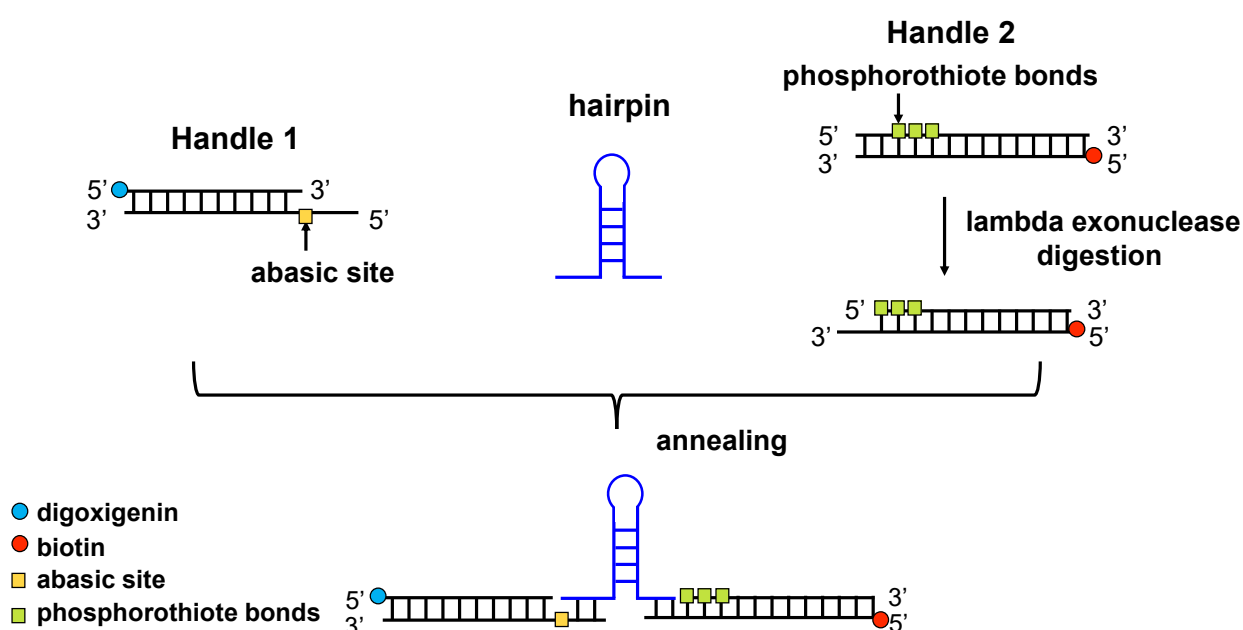


**Fig. S3** Schematic of DNA hairpin preparation.

DNA hairpin were generated as described previously<sup>3</sup>. In brief, DNA hairpin template consists of the ssDNA (to form hairpin) and two double-stranded DNA handles (“Handle 1” and “Handle 2”, see Fig. S3). Each handle included a single-stranded overhang complementary to one end of the ssDNA, and a biotin or digoxigenin modification at the opposite end that allowed the handle to be specifically linked to the antidigoxigenin-coated coverslip or streptavidin-coated 2.8  $\mu\text{m}$  paramagnetic beads (M270, Invitrogen). To create “Handle 1” with a 30-nt 5' overhang and a digoxigenin tag, a 1195 bp fragment from pJM1 plasmid was amplified by PCR

using forward primer Dig-H1F and reversed primer H1R containing an abasic site, shown in Table S1. A 1,410-bp handle with a 30-nt 3' overhang and a biotin label at the opposite end was prepared by PCR using H2F-3S primer containing three phosphorothioate bonds, one 5'-biotin modified primer Biotin-H2R, and the pJM1 plasmid as the template, followed by digestion with lambda exonuclease. Then after the purification of both two DNA handles (Qiagen, 28104), the ssDNA hairpin was annealed to these handles in annealing buffer (100 mM NaCl, 20 mM PIPES, pH 7.0 1 mM EDTA) with the ratio of 1:1:1, by lowering the temperature from 80 to 4 °C over 30 min.

## Section S2. Force calibration

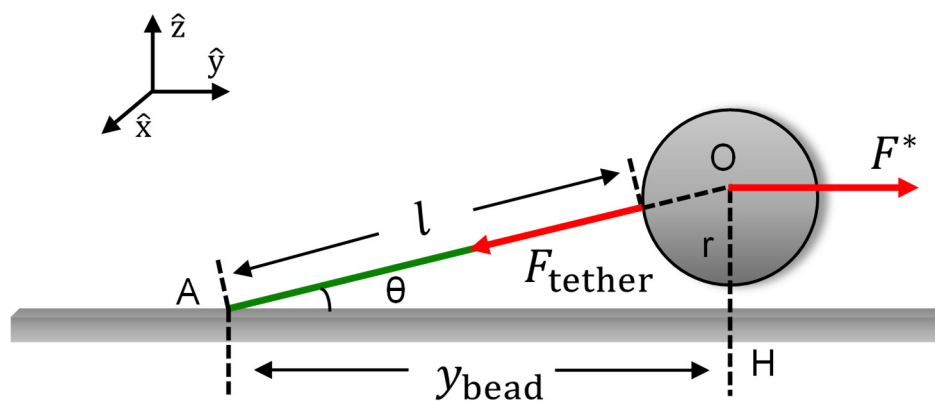


**Fig. S4** The geometric configuration of the DNA stretching in flow-cell

The force in flow-cell has been carefully quantified in the previous work <sup>4</sup> which showed that the calibrated force from the Brownian motion of the tethered bead has already included the contributions from both the hydrodynamic drag of DNA and the pulling force from the tethered bead. Fig. S4 is a cartoon of the geometric representation of the DNA stretching in flow-cell, and the flow rate is along the  $\hat{y}$  direction. Here, the Brownian motion of the tethered bead was analyzed in Fourier space. <sup>5-7</sup> The power spectral density of the bead fluctuations in  $x(t)$  can be fitted by Equation (S1), as shown in Fig. S5 (a)-(b)

$$p(f) = \frac{k_B T}{\pi^2 \beta (f_c^2 + f^2)} \quad (S1)$$

where  $k_B$  is Boltzmann's constant,  $T$  is the temperature,  $f_c$  is the cut-off frequency, and  $\beta$  is the friction coefficient of the bead. The stiffness of the system  $k$  can be derived by Equation (S2),

$$k = 2\pi\beta f_c \quad (S2)$$

The fluctuation of the tethered bead in  $\hat{x}$  direction can also be considered as a pendulum with an equivalent length of  $l + r$ , where  $r$  is the radius of the tethered bead.<sup>4, 8</sup> Thus, the equivalent stretching force on DNA  $F_{tether}$  and the equivalent hydrodynamic force  $F^*$  can be written as<sup>4</sup>,

$$F_{tether} = k(l + r) \quad (S3)$$

$$F^* = F_{tether} \cos \theta = k y_{bead} \quad (S4)$$

where  $l$  is the extension of the DNA,  $l = \sqrt{y_{bead}^2 + r^2} - r$ .

In the previous work<sup>4</sup>, it was found that  $F^*$  increased linearly with the increase of the volume flow rate  $V$ . Since  $\cos \theta$  changed slightly in our experiments, the relationship between  $F_{tether}$  and  $V$  were also approximately linear<sup>4</sup>,

$$F_{tether} = k_{tether} V \quad (S5)$$

The conversion factor  $k_{tether}$  was determined from the slope of the linear fitting, shown in Fig. S5 (c). Thus,  $F_{tether}$  can be calculated using Equation (S5) once  $k_{tether}$  was obtained. Fig. S5 (d) showed the distribution of  $k_{tether}$  calibrated from 106 different tethers forming by using the "Assisting-Force" DNA template and MyOne beads, where the Gaussian fitting yielded  $k_{tether} = 0.014 \pm 0.001$  pN min  $\mu\text{L}^{-1}$  (mean  $\pm$  S.D.).

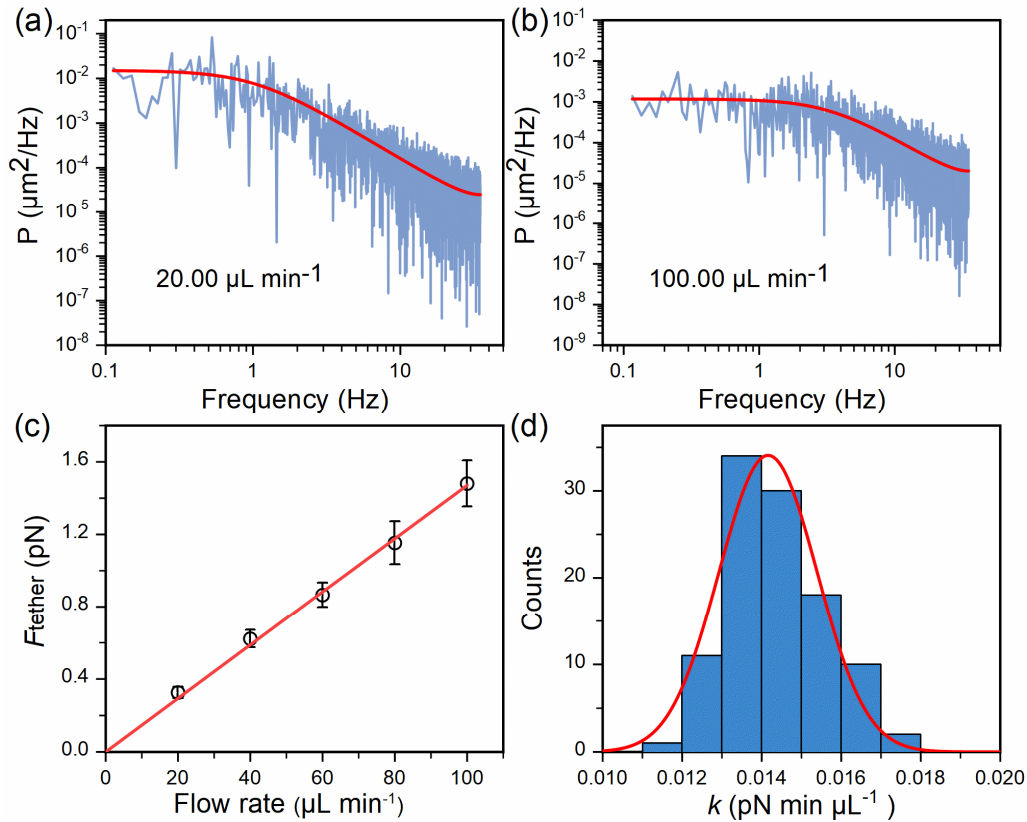


**Fig. S5** Calibration of the  $F_{tether}$  in Flow-cell. (a, b) The power spectrum of the Brownian motion of MyOne beads tethered with the “Assisting-Force” DNA template at a flow rate of  $20.00 \mu\text{L min}^{-1}$  (a) and  $100.00 \mu\text{L min}^{-1}$  (b). The fitting of the power spectrum (red line) yields  $F_{tether} = 0.3 \text{ pN}$  (a) and  $F_{tether} = 1.5 \text{ pN}$  (b), respectively. (c) Calibration of the relationship between  $F_{tether}$  and the volume flow rate  $V$ . The linear fitting (red line) of experiment data (black circle) yields the conversion factor  $k_{tether} = 0.015 \text{ pN min } \mu\text{L}^{-1}$ . (d) The distribution of  $k_{tether}$  obtained from 106 different tethers forming by the “Assisting Force” DNA template and MyOne beads. The Gaussian fitting yields  $k_{tether} = 0.014 \pm 0.001 \text{ pN min } \mu\text{L}^{-1}$  (mean  $\pm$  S.D.,  $N=106$ ).

### Section S3. Quantitative analysis of the fraction of stained DNA

Due to the influence of the fluorescence from the magnetic bead, the fraction of stained DNA during DNA stretching was calculated by the ratio of the length of stained DNA to the total length of stained and unstained DNA in the unaffected region. Specifically, a proper grayscale threshold  $I_t$  was selected to obtain the binary image. The number of pixels ( $N$ ) with their grayscale values greater than  $I_t$  along DNA was

counted, which indicated the length of stained DNA. To avoid the influence of the fluorescence from the magnetic bead, only the left part of DNA was analyzed, as indicated by  $L$  in Fig. S6 where  $L=L_0-D$ .  $D$  was the half length of the region affected by the fluorescence of the magnetic bead and  $L_0$  was the length measured from anchor point to the center of the tethered bead which was obtained by two-dimensional Gaussian fitting. In our analysis,  $D$  was set to be 40 pixels,  $N$  was counted for DNA in the range of  $L$  and the fraction of stained DNA was derived by  $N/L$ . Note here that  $L$  and  $L_0$  were also counted in pixels.

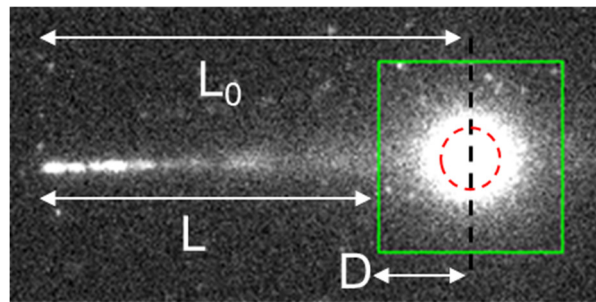


**Fig. S6 Analysis of the ratio of stained DNA.** The red dotted circle indicated the actual size of the M270 and the green box indicated the region affected by the fluorescence of the magnetic bead.  $D$  was set to be 40 pixels in the experiment.  $L_0$  was the length measured from anchor point to the center of the bead. To avoid the influence of the fluorescence from the magnetic bead during quantification of the fraction of strained DNA, only the left part of DNA was analyzed, indicated as  $L$ .



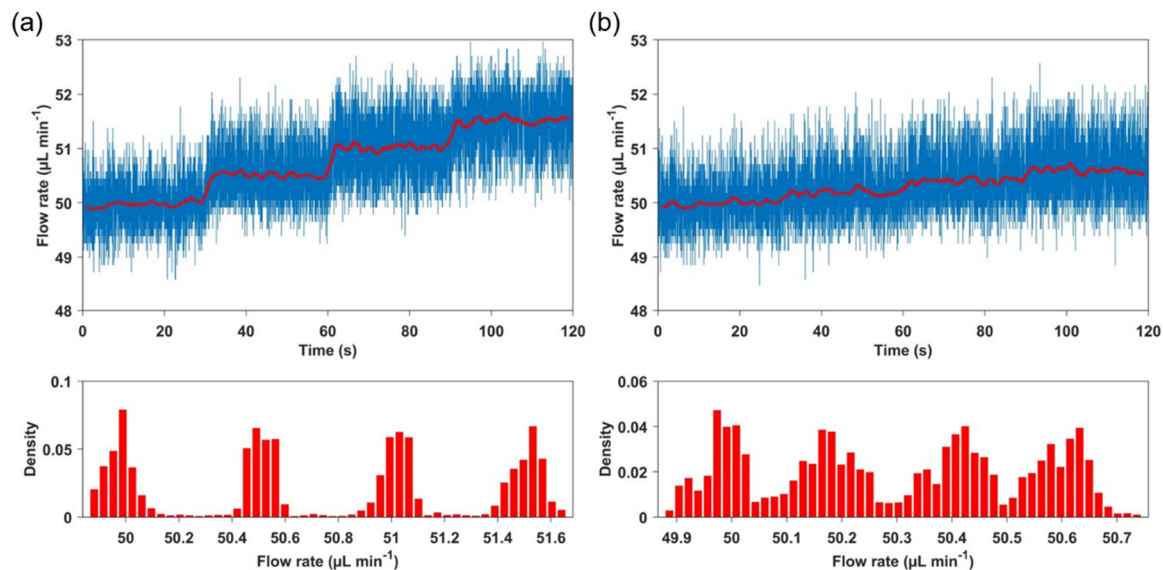


**Fig. S7** The resolution of the volume flow rate controlled by the gas-pump system. The flow rate increased from 50.00  $\mu\text{L min}^{-1}$  to 51.50  $\mu\text{L min}^{-1}$  at a step of 0.50  $\mu\text{L min}^{-1}$  (a) and from 50.00  $\mu\text{L min}^{-1}$  to 50.60  $\mu\text{L min}^{-1}$  at a step of 0.20  $\mu\text{L min}^{-1}$  (b) every 30 seconds. The raw data was sampled at 100 Hz (blue line) and smoothed to 0.5 Hz (red line). The distributions of smoothed flow rate shown in lower panels of (a) and (b). Four peaks were clearly identified at about 50.00  $\mu\text{L min}^{-1}$ , 50.50  $\mu\text{L min}^{-1}$ , 51.00  $\mu\text{L min}^{-1}$ , 51.50  $\mu\text{L min}^{-1}$  in (a) and 50.00  $\mu\text{L min}^{-1}$ , 50.20  $\mu\text{L min}^{-1}$ , 50.40  $\mu\text{L min}^{-1}$ , 50.60  $\mu\text{L min}^{-1}$  in (b), respectively. This result indicated that the resolution of the flow rate is very high in our flow-cell system and hence the force can be finely and precisely controlled.

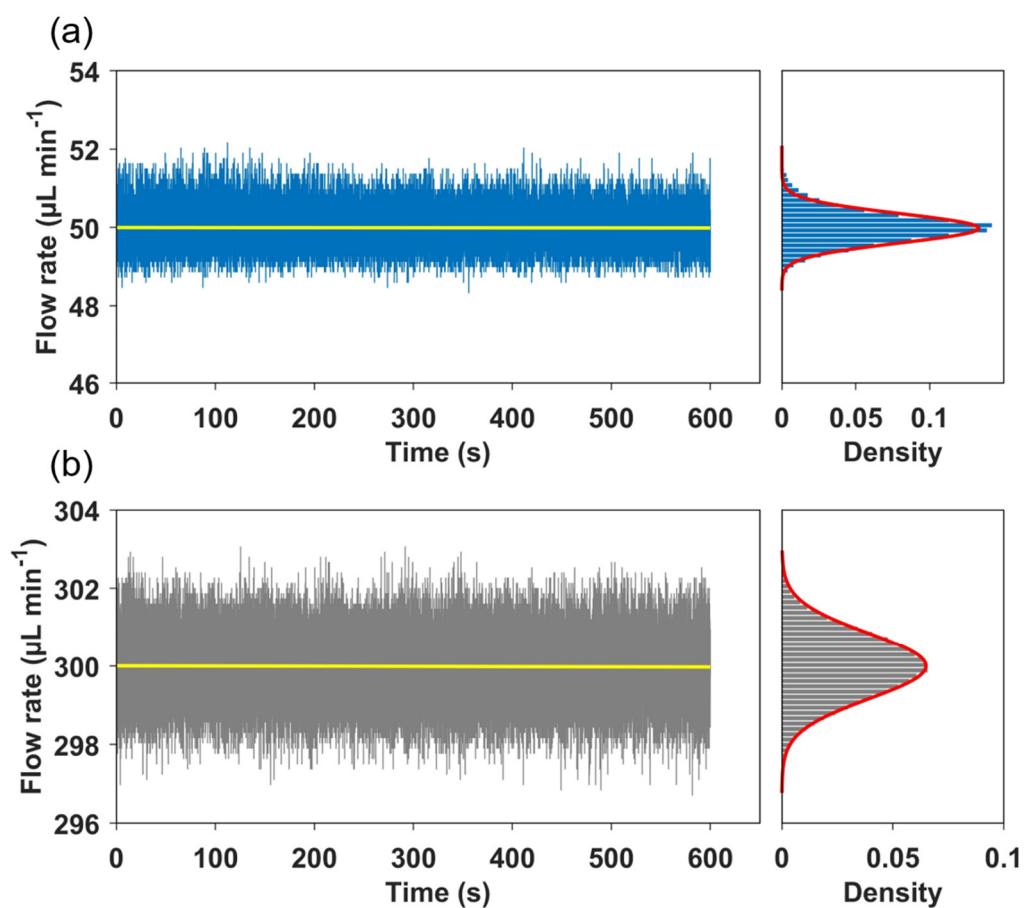


**Fig. S8** The long-term stability of flow rate for the flow cell measured at  $50.00 \mu\text{L min}^{-1}$  (a) and  $300.00 \mu\text{L min}^{-1}$  (b) for 10 minutes. The distributions of the raw data and the Gaussian fitting (red line) are shown in the right panels, from which the standard deviation and the coefficient of variation obtained were  $0.37 \mu\text{L min}^{-1}$  and  $0.74\%$  (a) and  $0.84 \mu\text{L min}^{-1}$  and  $0.28\%$  (b), respectively. The linear fittings (yellow line) of the raw data yielded the slope  $k = -2.1 \times 10^{-5} \mu\text{L min}^{-1} \text{s}^{-1}$  (a) and  $k = -5.3 \times 10^{-5} \mu\text{L min}^{-1} \text{s}^{-1}$  (b), which indicated that the drifting rates of flow rate were very small (*i.e.*,  $-0.01 \mu\text{L min}^{-1}$  per 10 min in a and  $-0.03 \mu\text{L min}^{-1}$  per 10 min in b) and can be ignored in general. Data was sampled at 100 Hz.

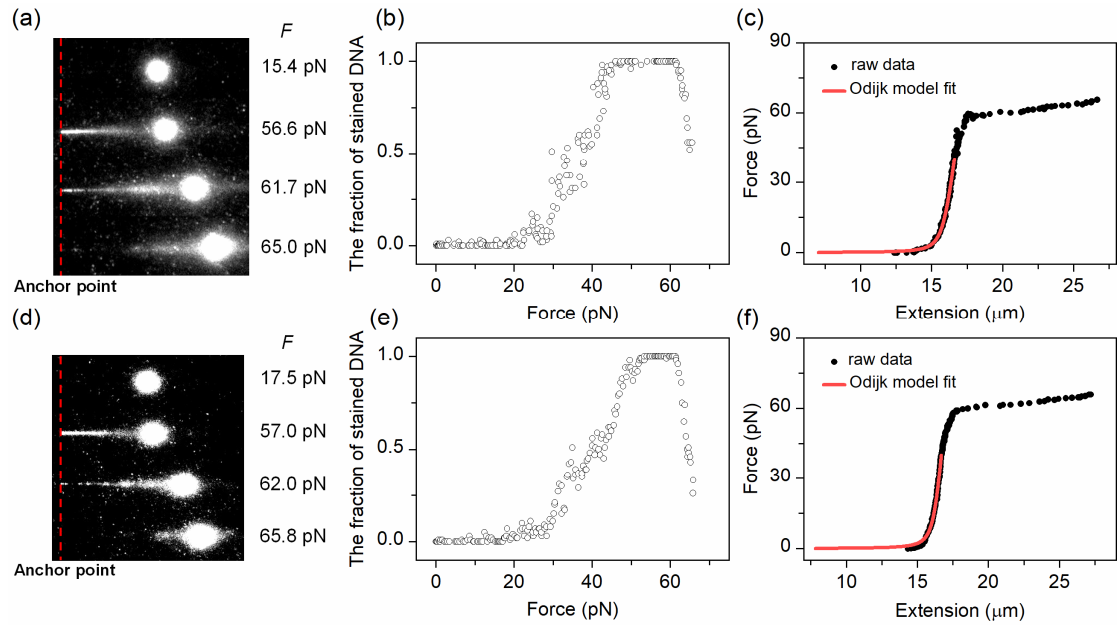


**Fig. S9** More traces and results for lambda DNA stretching with 5 nM SYTOX Orange using flow-cell. (a-c) The experimental results for one tether. (a) Fluorescence images of a lambda DNA tether under different forces. (b) The fraction of stained DNA plotted as a function of force. (c) The force-extension curve (FEC) (black solid dots) for lambda DNA measured by flow-cell. The Odijk WLC model fitting (red line) yielded contour length  $L_0 = 16334$  nm, persistence length  $L_p = 39$  nm, and stretching modulus  $K_0 = 942$  pN. (d-f) The experimental results for another tether. The Odijk WLC model fitting in (f) (red line) yielded  $L_0 = 16657$  nm,  $L_p = 45$  nm, and  $K_0 = 1553$  pN.

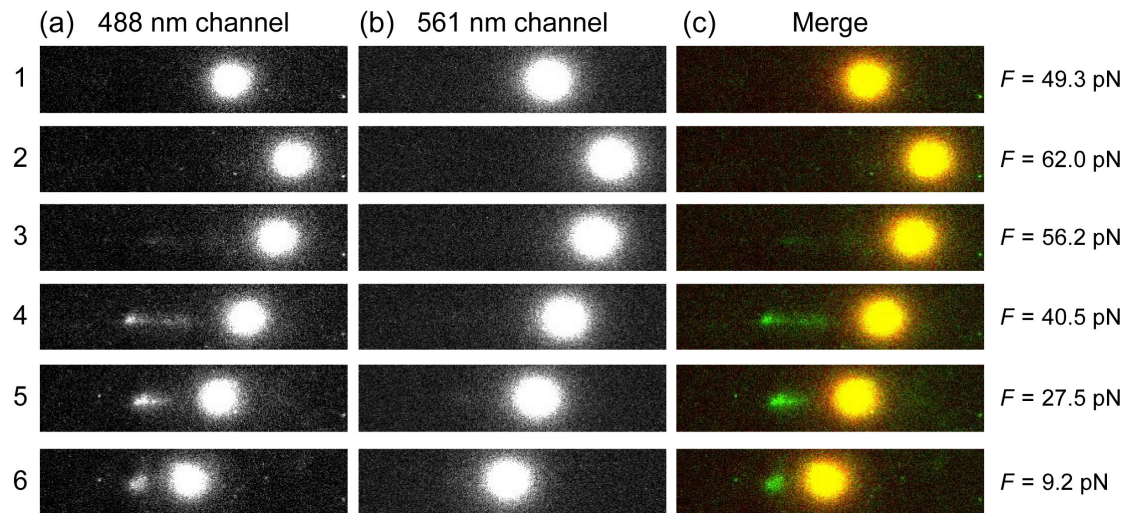


**Fig. S10** Fluorescence images of single stretched lambda DNA with 5 nM sfGFP-*EcoSSB* when 488-nm laser and 561-nm laser were simultaneously excited. (a, b) The fluorescence images were recorded in 488-nm (a) channel and 561-nm (b) channel, respectively. The first two rows, indicated as No.1 and 2, were acquired at the DNA stretching process and the last four rows, indicated as No. 3, 4, 5 and 6, were acquired at the relaxation process.

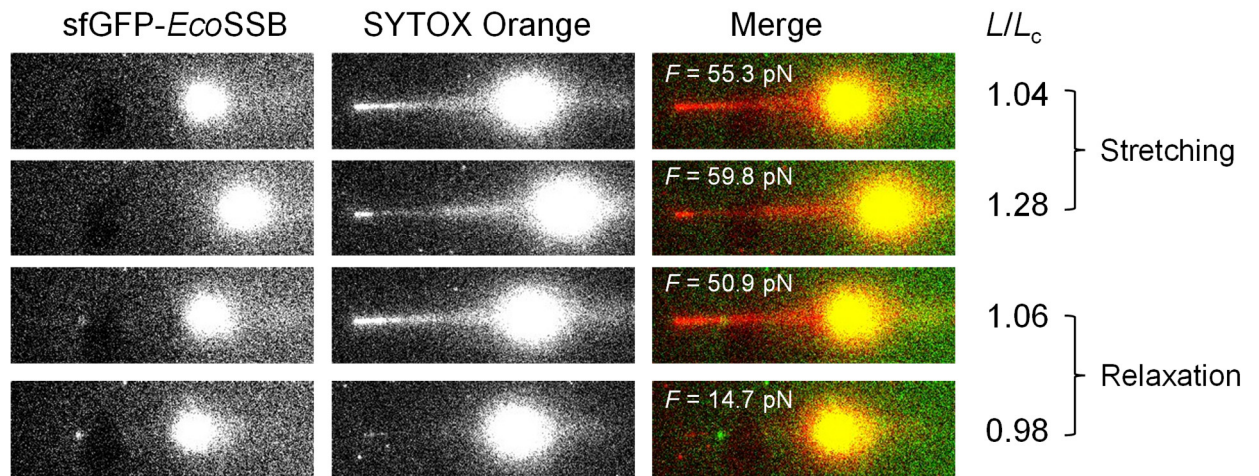


**Fig. S11** Fluorescence images of sfGFP-*Eco*SSB and SYTOX Orange binding to another stretched lambda DNA molecule. The DNA was imaged using 5 nM sfGFP-*Eco*SSB and 3 nM SYTOX Orange. Images of the left and central columns were acquired from SSB image channel and SYTOX Orange image channel of the Prime 95B, and merged together to obtain the image of the right column where the *Eco*SSB and SYTOX Orange molecules were indicated as green and red, respectively. Each row was measured under a different force, *i.e.*,  $F = 55.3$  pN,  $59.8$  pN,  $50.9$  pN,  $14.7$  pN from top to bottom.  $L/L_c$  indicated the ratio of measured length of lambda DNA to the theoretical contour length. The first two rows were acquired during DNA stretching and the last two rows were acquired during DNA relaxation.

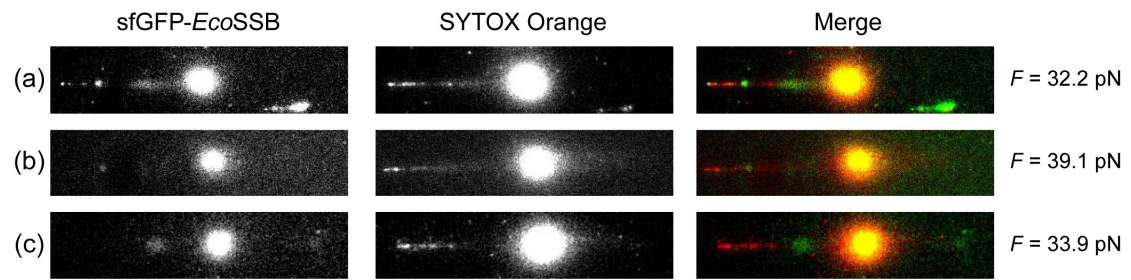


**Fig. S12** Fluorescence images of lambda DNA during the next round of stretching after experiencing overstretching transition and relaxation. (a-c) Fluorescence images for three different lambda DNA molecules.

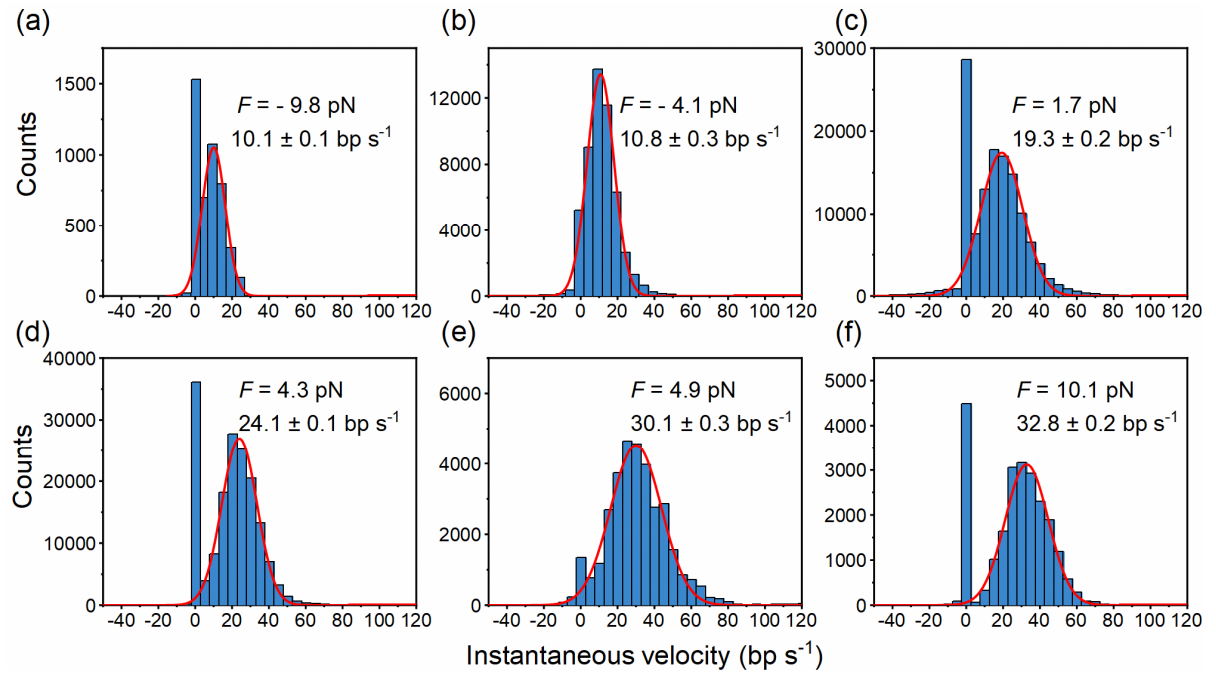


**Fig. S13** Distributions of pause-free velocities of T7 RNAP under different forces at 20 °C with 30 μM NTPs. Each distribution was fitted by a Gaussian function (solid red line) with its mean value and standard error indicated.



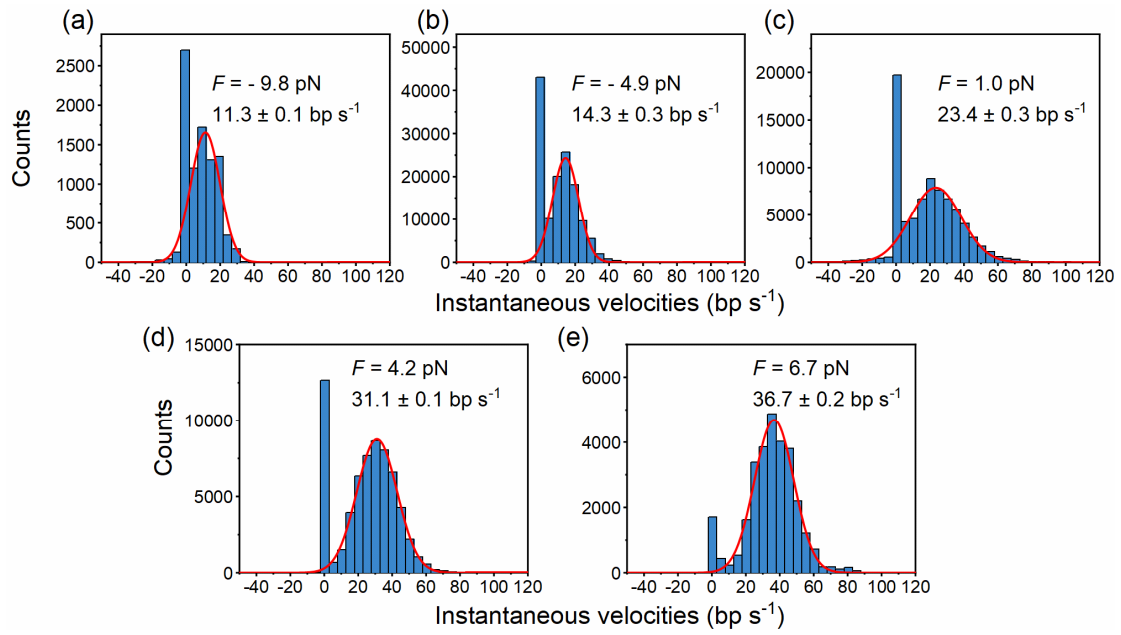


**Fig. S14** Pause-free velocities of T7 RNAP under different forces at 23 °C with 30 μM NTPs. Each distribution was fit by a Gaussian function (solid red line) with its mean value and standard error indicated.



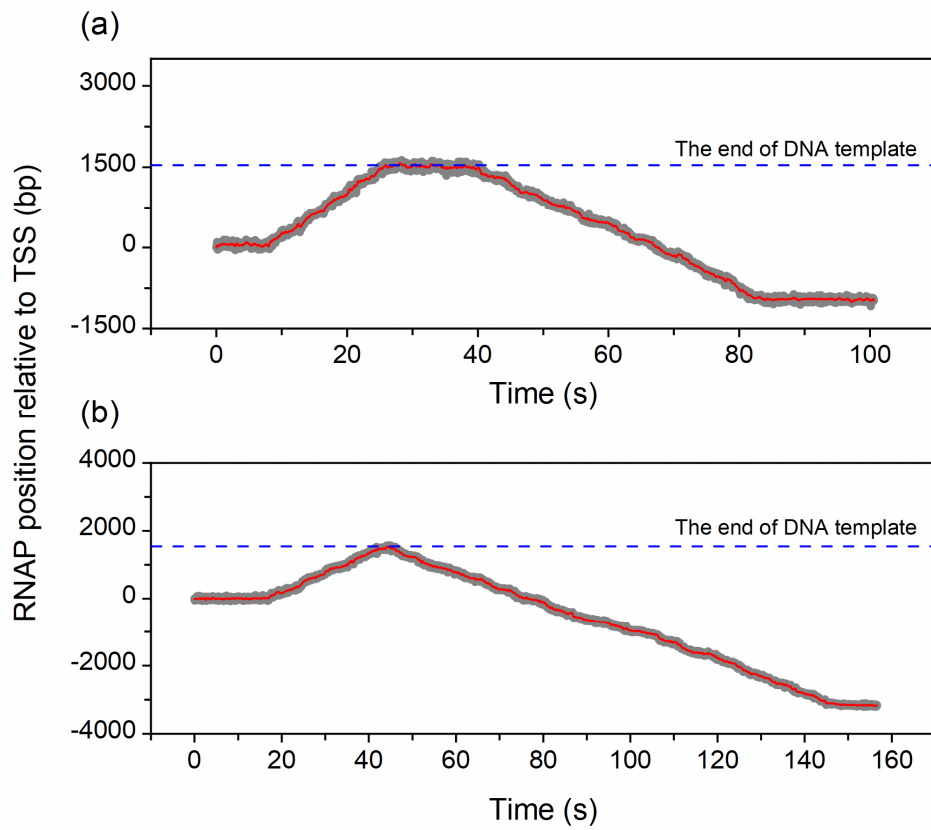


**Fig. S15** More traces of T7 RNA polymerase antisense transcription observed by flow-cell. (a, b) The data was measured under 4.5 pN at 20 °C with 300  $\mu$ M NTPs. Raw data were sampled at 33 Hz (gray) and then filtered to 5 Hz to get the smoothed data (red).

**Table S1.**

List of DNA oligomers used in sample preparation. All DNA oligomers were purchased from Sangon (Shanghai, China).

Experiments	Name	Sequence (5'-3')
DNA hairpin	Dig-H1F	/Dig/ATAGACAGATCGCTGAGATAGGTGCC
	H1R	AAGCTTGGCGTAATCATGGTCATAGCTGTT_CCTGTGTGAAAT TGTTATCCGCTCACAAT
	H2F-3S	/5Phos/CTAGAGGATCCCCGGGTACCGAGCTCGAATT*C*A*C
	Biotin-H2R	/Biotin/GAAGCATTATCAGGGTTATTGT CTCATGAGCGGATAACA
	DNA hairpin	AACAGCTATGACCATGATTACGCCAAGCTT_GAGTCCTGGAT CCTATTTTTAGGATCCAGGACTC_CTAGAGGATCCCCGGGTAC CGAGCTCGAAT
Multiple labeled lambda DNA	HAF4	CGTGGGTCTCGCGGTATCATTG
	HBR4	GGATCTCAAGAAGACCCTTTGATCTT
	Dig adaptor oligo 1	/5Phos/CAAAGCATTCCGGAAGCTCTGGACGT
	Dig adaptor oligo 2	/5Phos/AGGTCGCCGCCACGTCCAGAGCTTCCGAATGC
	biotin adaptor oligo 1	/5Phos/GGGCGGCGACCTGCATTCCGGAAGCTCTGGACGT
	biotin adaptor oligo 2	/5Phos/ACCGACGTCCAGAGCTTCCGAATGC
Assisting Force template	Assisting Force Forward	/Dig/CACTACCTGTCTGCTATCG
	Assisting Force Reverse	CGTTAGTCTGTGCGTACAC
Resisting Force template	Resisting Force Reverse	/Dig/GCTCCTTTGCTTTCTTC
	Resisting Force Forward	AGACGCCTTGTTGTTAGC

'\_' represents abasic site, '/5Phos/' represents that 5' end of the oligomer was phosphorylated, '/Dig/' represents that 5' end of the oligomer was digoxigenin labeled, '/Biotin/' represents that 5' end of the oligomer was biotin labeled, '\*' represents phosphorothioate bond.

### **Movie S1.**

The video of the lambda DNA overstretching with 1 nM SYTOX Orange.

### **Movie S2.**

The video of the lambda DNA overstretching with the 5 nM *E.coli* SSB (green) and 3 nM SYTOX Orange (red).

### **Movie S3.**

The video of the second round of lambda DNA stretching after it has been overstretched in the first round with the 5 nM *E.coli* SSB (green) and 3 nM Sytox orange (red).

### **References**

1. D. R. Burnham, H. B. Kose, R. B. Hoyle and H. Yardimci, *Nat. Commun.*, 2019, **10**, 2159.
2. P. Thomen, P. J. Lopez, U. Bockelmann, J. Guillerez, M. Dreyfus and F. Heslot, *Biophys J*, 2008, **95**, 2423-2433.
3. P. C. Anthony, C. F. Perez, C. García-García and S. M. Block, *Proc. Natl. Acad. Sci. U. S. A.*, 2012, **109**, 1485-1489.
4. J. Liang, J. Li, Z. Zhong, T. Rujiralai and J. Ma, *Nanoscale*, 2021, **13**, 15916-15927.
5. K. C. Neuman and S. M. Block, *Rev. Sci. Instrum.*, 2004, **75**, 2787-2809.
6. A. J. te Velthuis, J. W. Kerssemakers, J. Lipfert and N. H. Dekker, *Biophys J*, 2010, **99**, 1292-1302.
7. P. Daldrop, H. Brutzer, A. Huhle, D. J. Kauert and R. Seidel, *Biophys. J.*, 2015, **108**, 2550-2561.
8. H. Chen, H. Fu, X. Zhu, P. Cong, F. Nakamura and J. Yan, *Biophys J*, 2011, **100**, 517-523.